Potential energy surfaces of several van der Waals complexes modelled using distributed multipoles

3 AUTHORS:

David J. Wales
University of Cambridge
381 PUBLICATIONS **16,113** CITATIONS

SEE PROFILE

Anthony John Stone
University of Cambridge
135 PUBLICATIONS **9,534** CITATIONS

SEE PROFILE

Paul L A Popelier
The University of Manchester
190 PUBLICATIONS **7,115** CITATIONS

SEE PROFILE

Potential energy surfaces of several van der Waals complexes modelled using distributed multipoles

David J. Wales, Anthony J. Stone, Paul L.A. Popelier

University Chemical Laboratories, Lensfield Road, Cambridge CB2 1EW, UK

Received 11 November 1994; in final form 27 April 1995

Abstract

We report analyses of the potential energy surfaces of five van der Waals complexes, $Ar-NH_3$, $((CH_3)_2NH)_2$, propene$-SO_2$, acetylene$-N_2$ and acetylene$-CO$ described by a potential based upon distributed multipoles for the electrostatics and atom–atom Lennard-Jones terms for the dispersion–repulsion. In particular we describe the low energy rearrangement mechanisms in each system, and compare these results with those of previous studies, especially experimentally observed tunnelling splittings. Our results are mixed, probably due to the description of the dispersion–repulsion terms, although even in the worst cases the structures we find will serve as useful starting points for ab initio work. Improvement of the dispersion and repulsion terms in acetylene$-N_2$ and acetylene$-CO$ gives much better results.

1. Introduction

The electrostatic contribution to intermolecular binding may often determine the principal geometrical features of van der Waals complexes [1]. Distributed multipole analysis [2–4] (DMA) provides an accurate description of this term, which overcomes the convergence problems of a single centre expansion, and has been used successfully by Buckingham and Fowler in previous work [5]. We have developed a computer code which can calculate the analytic first and second derivatives of the zeroth-order electrostatic energy for distributed multipoles up to and including rank four, and have used it to study a variety of complexes [6–8]. In this Letter we consider five systems that have recently been the subject of experimental interest, namely $Ar-NH_3$, $((CH_3)_2NH)_2$, propene$-SO_2$, acetylene$-N_2$ and acetylene$-CO$. In each case the electrostatic DMA description is combined with Lennard-Jones atom–

atom terms for the dispersion and repulsion to give a qualitative but realistic intermolecular potential. In the present work we have also included the induction energy, iterated to convergence, for which the relevant derivatives have now been obtained.

The availability of analytic first and second energy derivatives enables us to employ eigenvector-following [9] to search routinely for transition states and minima, and to calculate reaction pathways. The details have been given elsewhere [7,8], as have formulae for the energy derivatives [6,7].

2. Results

The five new examples considered here have been the subject of recent theoretical and experimental work. We characterise the rearrangements in terms of the stationary points involved, the barrier heights and three indices which provide additional informa-

Table 1
Ar–NH$_3$: energies (cm^{-1}), point groups (PG), non-zero normal mode frequencies (cm^{-1}), rotational constants (cm^{-1}) and components of the dipole moment, μ_i (D), along the inertial axes (in the same order as the rotational constants)

Label	Energy	PG	Frequencies	Rotational constants	μ_i
min1	−144.1947	C$_{3v}$	43.1, 43.1, 48.7	6.3222, 0.1121, 0.1121	1.87, 0.00, 0.00
min2	−115.4725	C$_{3v}$	41.4, 50.0, 50.0	6.3223, 0.1028, 0.1028	1.87, 0.00, 0.00
ts1	−100.7333	C$_s$	18.5i, 39.6, 67.7	9.1041, 0.0944, 0.0944	0.75, 0.00, 1.72

tion about the path. The first is $S = \int ds$, the integrated arc length in $3N$-dimensional nuclear configuration space, where N is the number of atoms. The moment ratio of displacement, γ, was introduced by Stillinger and Weber [10]. We prefer to use the quantity $\tilde{N} = N/\gamma$, which is a measure of the number of atoms involved in the rearrangement. If a single atom moves then $\tilde{N} = 1$ and the rearrangement is localised, while if all atoms move through the same distance then $\gamma = 1$ and the process is entirely cooperative, with $\tilde{N} = N$. Finally, the distance between minima in nuclear configuration space [11], D, also provides insight, where $D \leqslant S$. The

Fig. 1. Rearrangement from the higher energy minimum found for Ar–NH$_3$ to the global minimum via a transition state in which the Ar atom passes over an H–H 'edge'. Distances are marked in bohr. The dashed lines in this figure are intended only to guide the eye and were generated with Mathematica [18] using a simple distance cut-off.

DMA calculations were carried out for DZP basis sets including the second-order Møller–Plesset correlation correction [12], unless stated otherwise. In each case the rigid molecule geometry is that obtained by optimisation at the same level of theory and we truncate the distributed multipoles after the hexadecapole ($L = 4$). The Lennard-Jones parameters employed were all obtained from Allen and Tildesley [13] and standard combination rules.

3. Ar–NH$_3$

There are two recent experimental investigations of the rearrangement barriers in this system [14–15]. We located two minima and one transition state as detailed in Table 1. Our DZP basis employed the Dunning double zeta combinations [16] with polarization functions having exponents of 0.8 for N and 1.0 for H. Point polarizabilities were assigned to the Ar atom (magnitude 11.08 atomic units) and to the centre of mass of the ammonia molecule ($\alpha_\perp = 14.33$ and $\alpha_\parallel = 16.27$ atomic units [17]). We find a global minimum with C$_{3v}$ symmetry where the Ar atom lies closer to the nitrogen atom than the three hydrogens. The saddle-point ts1, which is a C$_s$ structure in which the Ar atom bridges an H–H edge, links this structure to min2 in which the Ar atom occupies the other C$_{3v}$ site (Fig. 1 and Table 2). The rotational constants and dipole moment components along the inertial axes are also given in Table 1.

Previous experimental and theoretical results agree that the global minimum for this system is T-shaped
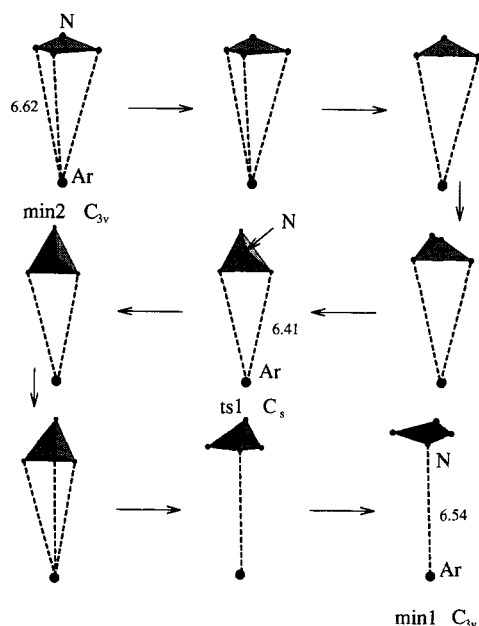
Table 2
Rearrangement pathways of Ar–NH$_3$. Energies are in cm^{-1} and S and D (defined in Section 2) are in bohr

E_1	Δ_1	E_{ts}	Δ_2	E_2	S	D	$\tilde{N}$
−144.1947	43.461	−100.7333	14.739	−115.4725	3.9	2.5	2.9

Table 3
Dimethylamine dimer: energies (cm^{-1}), point groups (PG), non-zero normal mode frequencies (cm^{-1}), rotational constants (cm^{-1}) and components of the dipole moment, μ_i (D), along the inertial axes (in the same order as the rotational constants)

Label	Energy	PG	Frequencies	Rotational constants	μ_i
			experiment:	0.1464, 0.0487, 0.0391	1.50, 0.00, 0.84
min1	− 1262.40	C_1	27.9, 40.2, 58.2, 67.4, 92.5, 172.3	0.1426, 0.0457, 0.0388	2.06, 0.58, 0.95
min2	− 1168.50	C_1	13.3, 26.5, 47.1, 55.9, 73.9, 161.2	0.1526, 0.0395, 0.0338	1.61, 0.29, 1.56
ts1	− 1166.37	C_1	12.4i, 29.7, 48.1, 59.2, 74.1, 161.0	0.1523, 0.0393, 0.0345	1.65, 0.40, 1.52
ts2	− 1148.05	C_s	12.9i, 19.5, 33.8, 68.0, 113.7, 149.1	0.1465, 0.0414, 0.0342	0.94, 0.00, 0.88
ts3	− 1141.24	C_s	17.6i, 15.4, 30.2, 51.7, 61.6, 178.9	0.1460, 0.0422, 0.0348	1.77, 0.00, 1.65

with the line joining the two centres of mass roughly perpendicular to the NH_3 C_3 axis and the Ar atom lying in a mirror plane equidistant from two H atoms [15,19–21]. However, Schuttenmaer et al. [15] find that the geometry corresponding to our global minimum lies some 40 cm^{-1} above the T-shaped minimum with the other C_{3v} geometry lying 50 cm^{-1} above. They calculate a barrier of about 28 cm^{-1} for internal rotation of NH_3. Grushow et al. have deduced a barrier height of 25.6 cm^{-1} for this parameter [14]. They also find that neither C_{3v} structure corresponds to a minimum.

Hence, although we find a T-shaped stationary point it corresponds to a transition state for the current potential. The surface is practically unchanged if we use multipoles calculated with a 6-31G$^{* *}$ basis and omit the MP2 correction. Hence we ascribe the observed deviation to the simplistic representation of the dispersion–repulsion energy.

4. The dimethylamine dimer

Tubergen and Kuczkowski [22] have recently studied the dimethylamine dimer using high resolution microwave spectroscopy. Their investigation was motivated by the considerable experimental and theoretical effort devoted to the ammonia dimer, in the
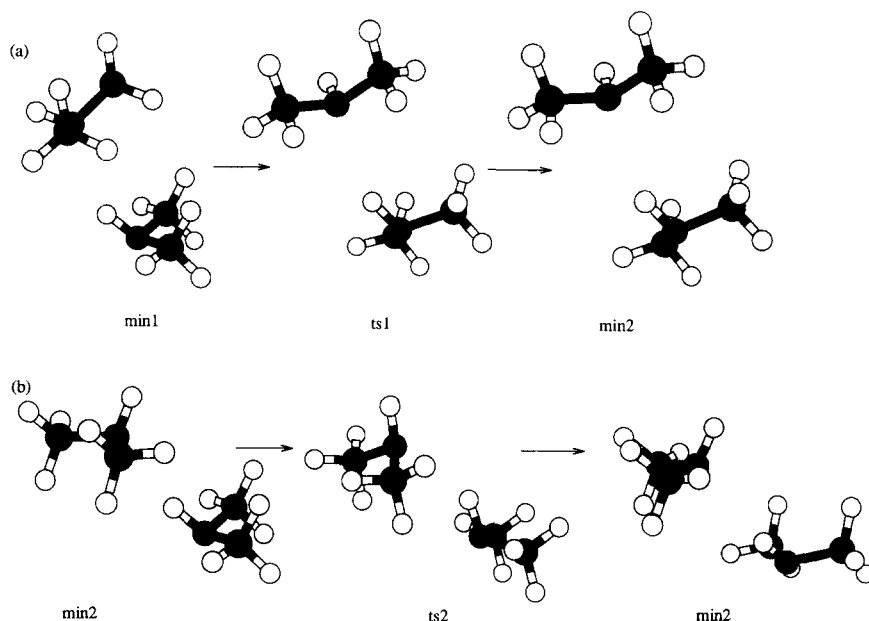

Fig. 2. (a) Rearrangement between the two lowest minima found for dimethylamine dimer. (b) Degenerate rearrangement of min2 for dimethylamine dimer via ts2 which possesses an additional plane of symmetry. These figures were produced with xmol [23].

Table 4

Rearrangement pathways of dimethylamine dimer. Energies are in cm^{-1} and S and D (defined in Section 2) are in bohr.

E_1	Δ_1	E_{ts}	Δ_2	E_2	S	D	$\tilde{N}$
−1262.4068	96.04	−1166.37	2.14	−1168.51	7.4	6.8	14.7
−1168.5061	20.46	−1148.05	20.46	−1168.51	8.0	4.8	12.6
−1168.5061	27.26	−1141.25	27.26	−1168.51	6.1	4.7	15.3

hope that this related system might be equally interesting. Using isotopic substitution they obtained sufficient experimental information to rule out many possible dimer geometries for $((CH_3)_2NH)_2$ and concluded that the most likely structures have nonlinear hydrogen bonds. On the basis of ab initio calculations and a distributed multipole analysis to estimate the electrostatic energy they finally concluded that one particular structure is the most plausible.

We found two minima and three transition states for this complex (Table 3). Our DZP basis employed the Dunning double zeta combinations [16] with polarization functions having exponents of 0.8 for N and C and 1.0 for H. Point polarizabilities were assigned to the centre of mass of each molecule using values calculated within the same ab initio DZP/MP2 formalism. The lowest energy minimum has a structure not considered by Tubergen and Kuczkowski, with the two molecules in similar parallel orientations (Fig. 2a). The rotational constants of this structure match the experimental values quite well, and the dipole moment components are reasonable. However, the other minimum, which appears to correspond to structure 3A of Tubergen and Kuczkowski [22], matches the dipole moments somewhat better but not the rotational constants. The two

minima can interconvert via ts1, as shown in Fig. 2a, and there are two relatively low energy rearrangements of min2, one of which is shown in Fig. 2b (see also Table 4). The apparent lack of a low-energy degenerate rearrangement might explain the failure of experiment to find tunnelling splittings [22]. However, Muguet et al. [24] have noted that this might also occur if the barrier is small.

5. Propene–sulphur dioxide

Eight isotopomers of propene–SO$_2$ have recently been studied by Xu and Kuczkowski [25] using microwave spectroscopy. From fitting the rotational constants they deduced that the complex has a stacked, near parallel planes configuration with a centre-of-mass distance of 3.26 Å, dipole moment of magnitude 1.34 D and binding energy 1014 cm^{-1}. Two reasonable structures resulted from least-squares fitting of the structural data, but one of these was eliminated on the basis of the dipole moment, ab initio results and calculations of the electrostatic energy using a distributed multipole analysis [25].

Our DZP basis employed the Dunning double zeta combinations [16] with polarization functions having exponents of 0.8 for C, 1.0 for H, 0.65 for S and 0.9 for O. Point polarizabilities were placed at the centres of mass using tabulated values [17] for SO$_2$ and values calculated within the same ab initio DZP/MP2 formalism for propene. We found two minima and four transition states for this system, as detailed in Table 5. The four rearrangements are summarised in Table 6. We did not find any low energy pathways corresponding to degenerate rear-

Table 5

Propene–sulphur dioxide: energies (cm^{-1}), point groups (PG), non-zero normal mode frequencies (cm^{-1}), rotational constants (cm^{-1}) and components of the dipole moment, μ_i (D), along the inertial axes (in the same order as the rotational constants)

Label	Energy	PG	Frequencies	Rotational constants	μ_i
			experiment:	0.1424, 0.0526, 0.0490	0.48, 0.70, 1.04
min1	−1584.45	C$_1$	28.2, 63.7, 77.4, 95.2, 122.1, 129.4	0.1390, 0.0530, 0.0517	0.51, 0.71, 0.97
min2	−1420.97	C$_1$	13.8, 61.0, 76.5, 85.1, 100.8, 137.9	0.1491, 0.0531, 0.0428	0.18, 0.40, 1.75
ts1	−1417.59	C$_1$	14.5i, 59.8, 79.3, 84.6, 100.9, 138.0	0.1467, 0.0527, 0.0426	0.08, 0.16, 1.67
ts2	−1346.28	C$_1$	13.3i, 47.9, 63.6, 74.3, 114.7, 135.2	0.1459, 0.0480, 0.0458	0.57, 0.93, 1.74
ts3	−898.59	C$_1$	50.5i, 15.6, 40.2, 63.8, 72.1, 77.3	0.1829, 0.0405, 0.0354	1.22, 0.85, 0.19
ts4	−484.71	C$_s$	31.5i, 20.4, 42.1, 60.5, 62.4, 68.2	0.1717, 0.0320, 0.0271	1.38, 0.95, 0.00

Table 6
Rearrangement pathways of propene–sulphur dioxide. Energies are in cm^{-1} and S and D (defined in Section 2) are in bohr

E_1	Δ_1	E_{ts}	Δ_2	E_2	S	D	$\tilde{N}$
−1584.45	166.87	−1417.5863	3.39	−1420.97	4.4	4.0	9.1
−1584.45	238.17	−1346.2826	74.69	−1420.97	12.5	9.6	9.0
−1584.45	685.86	−898.5865	685.86	−1584.45	11.2	5.0	7.2
−1420.97	936.26	−484.7142	936.26	−1420.97	9.5	5.7	5.2

rangements in this case, but there are two pathways with relatively small barriers that link the two lowest minima, as illustrated in Fig. 3. From Table 5 we see that min1 matches the experimental data best, although the binding energy is probably too large. The dipole moment components are in particularly good agreement. The centre-of-mass separation is 3.21 Å for min1 and 3.37 Å for min2, which bracket the experimental number. Taking all the present results for a range of complexes into account we cannot safely assume that min2 really exists on the true potential energy surface. However, this possibility is worth investigating.

6. Acetylene–nitrogen

The complex of acetylene with molecular nitrogen is known to be linear, from both microwave [26] and infrared [27] spectroscopy. The microwave spectra of $^{14}N^{15}N$–HCCH and $^{15}N^{14}N$–HCCH are distinct, showing that any motion which exchanges the two N atoms is slow on the timescale of the microwave experiment. The infrared spectrum yields an approximate value of the van der Waals stretching frequency of 38 ± 4 cm^{-1}, and van der Waals frequencies of 20 and 30 cm^{-1} for the C bend and S bend, respectively.

A 6-31G* DMA-LJ description fails completely in this case, giving a T-shaped minimum at an energy of −367 cm^{-1} with the acetylene molecule forming the head of the T, and a T-shaped transition state with the N_2 forming the head of the T at −185 cm^{-1}. The linear configuration is repulsive at all distances. There is an X structure, with both molecules perpendicular to the line between their centres and to each other, but it is an index-2 station-
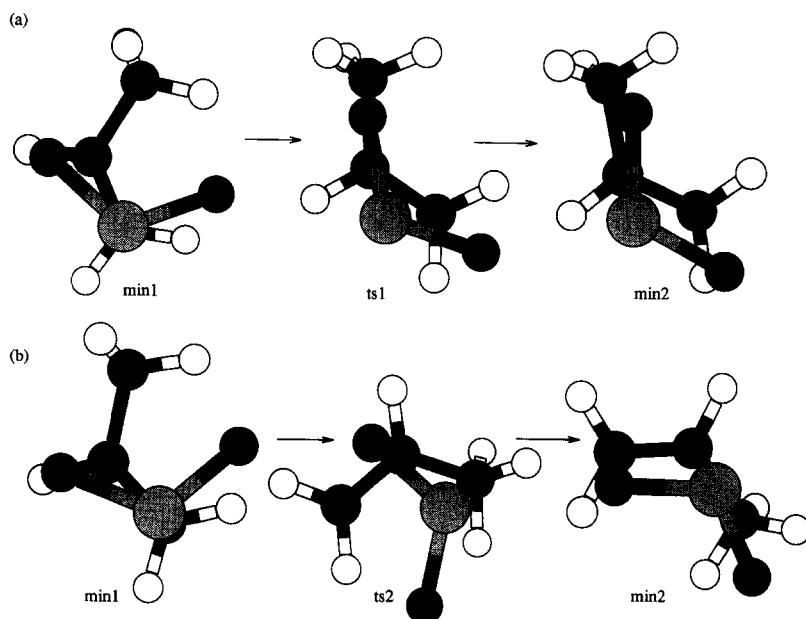

Fig. 3. Relatively low energy rearrangements from min1 to min2 via ts1 and ts2 for propene–SO_2. Min1 most closely matches the experimental results. These figures were prepared with xmol [23].

Table 7
Acetylene–N_2: energies (cm^{-1}), point groups (PG), non-zero normal mode frequencies (cm^{-1}), rotational constants (cm^{-1}) and components of the dipole moment, μ_i (D), along the inertial axes (in the same order as the rotational constants)

Label	Energy	PG	Frequencies	Rotational constants	μ_i
min1	−274.62	$C_{\infty v}$	14.1, 14.1, 56.8, 77.8, 77.8	∞, 0.0494, 0.0494	0.00, 0.00, 0.00
ts1	−207.92	C_{2v}	15.1i, 29.8, 47.9, 56.6	0.7085, 0.0881, 0.0783	0.00, 0.00, 0.00
ts2	−140.37	C_{2v}	27.2i, 20.3, 39.8, 43.1	0.7084, 0.0802, 0.0781	0.00, 0.00, 0.00

ary point with energy of -95 cm^{-1}. Rotating the molecules about the line of centres so that they become parallel gives another index-2 structure with a binding energy of only 29 cm^{-1}.

If the potential is improved the results are much better. The multipoles were calculated using a DZP basis sets at the MP2 level. The repulsion was described using an anisotropic exponential repulsion derived using the test particle method of Stone and Tong [28]. Dispersion (C_6) parameters were derived using a geometric-mean combining rule from the N...N parameters of Berns and Van der Avoird [29] and the hydrocarbon atom–atom parameters of Williams [30]. The induction energy was included, assigning half the experimental dipole polarizability of N_2 to each N atom and half the polarizability of acetylene to each C atom. This rather crude model is adequate in this case, as the induction energy is less than 10% of the other terms in magnitude.

This description, although still capable of improvement, appears to give a good account of the complex. The minimum structure is linear, with a binding energy of 275 cm^{-1} and a centre-of-mass separation of 4.86 Å, compared with the experimental separation of 4.82 Å. The van der Waals stretching frequency of about 57 cm^{-1} is somewhat larger than the experimental value, but is close to the value of 61 cm^{-1} obtained from SCF/MP2 calculations with a large basis set [31]. The van der Waals bending frequencies are calculated to be 14 cm^{-1} for the C bend and 78 cm^{-1} for the S-bend. Again,

these are quite close to the SCF/MP2 values of 23 and 75 cm^{-1}. There is a transition state in which the two molecules lie parallel to each other and perpendicular to the centre-of-mass vector. The barrier for motion of the N_2 molecule from one end of the acetylene to the other via this saddle point is 67 cm^{-1}, which does not conflict with the observation that HCCH...$^{14}N^{15}N$ and HCCH...$^{15}N^{14}N$, which would exchange by this path, are distinguishable in experiments at 5 K. There is another saddle-point, with a crossed structure, 134 cm^{-1} above the global minimum (Tables 7 and 8).

7. Acetylene–carbon monoxide

This complex too is linear [27], with a centre-of-mass separation of 5.011 Å. The van der Waals vibrational frequencies, in cm^{-1}, are estimated to be 48 ± 2 (stretch), 25 (C-bend) and 38 (S-bend). The 6-31G* DMA-LJ description performs badly here too. There is a linear HCCH–CO stationary point at -253 cm^{-1}; it has index-2 but the imaginary frequency is only 3.7 cm^{-1}. However the minimum is an approximately parallel structure with energy -435 cm^{-1}. The linear HCCH–OC structure is a true minimum, with an energy of -265 cm^{-1}.

As for HCCH–N_2, an improved potential gives much better results. The distributed multipoles were calculated at the DZP/MP2 level, and distributed polarizabilities for CO were taken from Ángyán et al. [32]. The repulsion potential was determined using the test-particle method [28], with the isotropic terms in the atomic radii adjusted slightly to give a centre of mass separation close to the experimental value.

The minimum energy HCCH...CO structure is linear, with a binding energy of 404 cm^{-1}. Optimization of a linear HCCH...OC structure leads to

Table 8
Rearrangement pathways of acetylene–N_2. Energies are in cm^{-1} and S and D (defined in Section 2) are in bohr

E_1	Δ_1	E_{ts}	Δ_2	E_2	S	D	$\bar{N}$
−274.62	66.70	−207.92	66.70	−274.62	8.9	5.3	3.0
−274.62	134.25	−140.37	134.25	−274.62	13.1	5.1	2.5

Table 9
Acetylene–CO: energies (cm^{-1}), point groups (PG), non-zero normal model frequencies (cm^{-1}), rotational constants (cm^{-1}) and components of the dipole moment, μ_i (D), along the inertial axes (in the same order as the rotational constants)

Label	Energy	PG	Frequencies	Rotational constants	μ_i
min1	−404.44	$C_{\infty v}$	19.4, 19.4, 61.8, 99.6, 99.6	∞, 0.0464, 0.0464	0.49, 0.10, 0.00
ts1	−157.12	C_s	30.4i, 28.3, 42.5, 50.5	0.7098, 0.0849, 0.0826	0.05, 0.00, 0.49
index-2	−119.34	$C_{\infty v}$	6.4i, 6.4i, 35.6, 35.6, 42.7	∞, 0.0500, 0.0500	0.49, 0.00, 0.00

Table 10
Rearrangement pathways of acetylene–CO. Energies in cm^{-1} and S and D (defined in Section 2) are in bohr

E_1	Δ_1	E_{ts}	Δ_2	E_2	S	D	$\bar{N}$
−404.44	247.33	−157.11	247.33	−404.44	12.1	5.1	2.5

an index-2 stationary point with a centre-of-mass separation of 4.82 Å and a binding energy of only 119 cm^{-1}. Full optimization from this geometry leads back to the HCCH...CO linear minimum, and we found no other stationary point except for a crossed structure at $-157\ cm^{-1}$, which is the transition state for the rearrangement of the CO from one end of the acetylene molecule to the other (Tables 9 and 10).

At the minimum, the centre-of-mass separation is 5.015 Å, compared with the experimental value of 5.011 Å [27], but this agreement was achieved by adjusting the repulsion term in the potential. The van der Waals stretching frequency is 62 cm^{-1}, compared with the experimental value of 48 cm^{-1}, and the bending frequencies are 19 and 100 for the C- and S-bends, respectively. As for HCCH–N_2, the C-bend frequency is reasonably close to the experimental value, but the S-bend frequency is too high. The intermolecular frequencies compare favourably with SCF/MP2 calculations with a large basis set [33], which give values of 39 and 108 cm^{-1} for the bends and 85 cm^{-1} for the stretch.

8. Conclusions

We have presented the lowest rearrangement pathways calculated for five van der Waals complexes using an intermolecular potential based upon distributed multipoles for the electrostatics and atom–atom Lennard-Jones terms for the dispersion

and repulsion terms. The agreement with previous theoretical and experimental results is variable, and we ascribe this mostly to the representation of the dispersion–repulsion energy rather than to the quality of the multipoles. The Berthelot rule, in particular, is known to give well depths between unlike atoms that are too deep [34]. We conclude that a relatively accurate potential energy surface will require a more sophisticated treatment of the offending terms. It may be significant that a number of spurious minima were found to disappear when the induction energy was included. The degree of cooperativity seen for the present rearrangements is in line with those reported elsewhere for a larger set of examples [8]: there does not appear to be a strong correlation with the barrier height, and localised processes are rare because the molecules must move as rigid bodies.

The results for HCCH...N_2 and HCCH...CO, which were obtained using a rather better potential model, are particularly encouraging, giving structures and intermolecular harmonic frequencies that are comparable in accuracy with those obtained from high-quality ab initio calculations.

References

[1] C.E. Dykstra, Chem. Rev. 93 (1993) 2339.
[2] A.J. Stone, Chem. Phys. Letters 83 (1981) 233;
    A.J. Stone and M. Alderton, Mol. Phys. 56 (1985) 1047.
[3] W.A. Sokalski and A. Sawaryn, J. Chem. Phys. 87 (1987) 526; J. Mol. Struct. 256 (1992) 91.
[4] F. Vigné-Maeder and P. Claverie, J. Chem. Phys. 88 (1988) 4934.

[5] A.D. Buckingham and P.W. Fowler, Can. J. Chem. 63 (1985) 2018;
P.W. Fowler and A.D. Buckingham, Chem. Phys. Letters 176 (1991) 11.

[6] P.L.A. Popelier and A.J. Stone, Mol. Phys. 97 (1994) 411.

[7] P.L.A. Popelier, A.J. Stone and D.J. Wales, Faraday Discussions 97 (1994) 243.

[8] D.J. Wales, P.L.A. Popelier and A.J. Stone, J. Chem. Phys. 102 (1995) 5556.

[9] J. Pancik, Collection Czech. Chem. Comm. 40 (1974) 1112;
C.J. Cerjan and W.H. Miller, J. Chem. Phys. 75 (1981) 2800.

[10] F.H. Stillinger and T.A. Weber, Phys. Rev. A 23 (1983) 2408.

[11] H. Tanaka and I. Ohmine, J. Chem. Phys. 91 (1989) 6318;
I. Ohmine and H. Tanaka, J. Chem. Phys. 93 (1990) 8138.

[12] C. Møller and M.S. Plesset, Phys. Rev. 46 (1934) 618.

[13] M. Allen and D.J. Tildesley, The computer simulation of liquids (Clarendon Press, Oxford, 1987).

[14] A. Grushow, W.A. Burns, S.W. Reeve, M.A. Dvorak and K.R. Leopold, J. Chem. Phys. 100 (1994) 2413.

[15] C.A. Schuttenmaer, R.C. Cohen and R.J. Saykally, J. Chem. Phys. 101 (1994) 146.

[16] T.H. Dunning, J. Chem. Phys. 53 (1970) 2823.

[17] C.G. Gray and K.E. Gubbins, Theory of molecular fluids, Vol. 1 (Clarendon Press, Oxford, 1984).

[18] S. Wolfram, Mathematica, 2nd Ed. (Addison-Wesley, New York, 1991).

[19] G. Chalisińsky, S.M. Cybulski, M.M. Szczęśniak and S. Scheiner, J. Chem. Phys. 91 (1989) 7809.

[20] M. Bulski, P.E.S. Wormer and A. Van der Avoird, J. Chem. Phys. 94 (1991) 491.

[21] F.M. Tau and W. Klemperer, J. Chem. Phys. 101 (1994) 1129.

[22] M.J. Tubergen and R.L. Kuczkowski, J. Chem. Phys. 100 (1994) 3377.

[23] xmol © 1990, 1991, 1992, 1993 Research Equipment, Inc., Minnesota Supercomputer Center, Inc.

[24] F.F. Muguet, G.W. Robinson and M.P. Bassez-Muguet, J. Chem. Phys. 102 (1995) 3655.

[25] L.-W. Xu and R.L. Kuczkowski, J. Chem. Phys. 100 (1994) 15.

[26] A.C. Legon, A.L. Wallwork and P.W. Fowler, Chem. Phys. Letters 184 (1991) 175.

[27] R.D. Beck, A.G. Maki, S.H. Tseng and R. Watts, J. Mol. Spectry. 158 (1993) 306.

[28] A.J. Stone and C.S. Tong, J. Comput. Chem. 15 (1994) 1377.

[29] R.M. Berns and A. Van der Avoird, J. Chem. Phys 72 (1980) 6107.

[30] D.E. Williams, J. Chem. Phys 45 (1965) 3770.

[31] S.A.C. McDowell and A.D. Buckingham, Chem. Phys. 171 (1993) 89.

[32] A.G. Ángyán, G. Jansen, M. Loos, C. Hättig and B.A. Heß, Chem. Phys. Letters 219 (1994) 267.

[33] S.A.C. McDowell and A.D. Buckingham, Chem. Phys. Letters 182 (1991) 551.

[34] G.C. Maitland, M. Rigby, E.B. Smith and W.A. Wakeham, Intermolecular forces (Clarendon Press, Oxford, 1981).